SANDIA REPORT

SAND88—1085 • UC—2
Unlimited Release
Printed May 1989

Stage Response of an Andersen Cascade Impactor to Monodisperse Droplets

D. J. Rader, L. A. Mondy, J. E. Brockmann, D. A. Lucero

Prepared by
Sandia National Laboratories
Albuquerque, New Mexico 87185 and Livermore, California 94550
for the United States Department of Energy
under Contract DE-AC04-76DP00789

Issued by Sandia National Laboratories, operated for the United States Department of Energy by Sandia Corporation.

Available to DOE and DOE contractors from
Office of Scientific and Technical Information
PO Box 62
Oak Ridge, TN 37831

Prices available from (615) 576-8401, FTS 626-8401

Available to the public from
National Technical Information Service
US Department of Commerce
5285 Port Royal Rd
Springfield, VA 22161

NTIS price codes
Printed copy: A02
Microfiche copy: A01

Distribution
UC–2

SAND88–1085
Unlimited Release
Printed May 1989

SAND--88-1085

DE89 014398

Stage Response of an Andersen Cascade Impactor to Monodisperse Droplets*

D.J. Rader, L.A. Mondy
Fluid and Thermal Sciences Department

J.E. Brockmann, D.A. Lucero
Reactor Safety Research Department

Sandia National Laboratories
Albuquerque, New Mexico, 87185

Abstract

Stage responses for an Andersen Mark III cascade impactor have been experimentally determined using monodisperse oil droplets. The impactor was operated upright and fully assembled so that interstage interference and wall losses could be properly studied. Interstage losses reached a maximum of about 15% for particle aerodynamic diameters of about 10 μm. The observed stage responses, defined as the fraction of particles entering the impactor that are collected on a stage, showed maxima that fell significantly short of unity (as low as 0.6). Physically, maxima less than unity indicate that a monodisperse aerosol is never collected exclusively on one stage, but is distributed among several stages and internal losses. Correlations for the stage responses are presented so that the experimental results can be used to determine size distributions with available data–inversion algorithms. One potential application of this technique is the characterization of droplet clouds generated by explosive events.

---

* This work was performed at Sandia National Laboratories supported by the U.S. Department of Energy under Contract DE—AC04—76DP00789

Contents

List of Figures

List of Tables

1 Introduction

Cascade impactors are widely used for the measurement of aerosol size distributions; their ruggedness and simplicity of operation make them an attractive choice in a variety of environments. In one common application, the aerosol of interest is drawn through the impactor, and the amount deposited on each stage is determined gravimetrically. The primary objective is to extract as much information as possible about the initial size distribution from the resulting set of weights. Unfortunately, the reconstruction of continuous size distributions from finite data sets is an ill–posed problem. Not surprisingly, a variety of such reconstruction techniques are presently in use; the success of each method depends on the particular nature of the aerosol sample and the instrument response.

These techniques all share the requirement that the response functions for each stage be known. The stage response function gives the fraction of particles entering the impactor that deposits on that stage. Values of the response function range from zero to one, and depend on impactor operating conditions (*e.g.*, geometry, flow rate, and gas properties) and particle properties (*e.g.*, diameter, density, and shape factor). As interstage interferences and particle losses will affect each stage's response, the response of each stage should be measured for a fully assembled impactor. Unfortunately, impactor stage response functions are rarely reported; rather, single–stage efficiency curves are given which provide an incomplete description of impactor performance.

This paper presents an experimental determination of the stage responses for a fully assembled Andersen Mark III cascade impactor (Andersen Samplers Inc., Atlanta, GA). Since our primary application is the measurement of the droplet distribution within an explosively–generated cloud, the calibration has been performed with monodisperse liquid droplets. Losses within the impactor are measured, and their treatment within data inversion techniques is discussed. In addition, correlations for the impactor response functions are presented so that the experimental results can be used to determine size distributions with available data–inversion algorithms.

2 Background

In a single–stage impactor, a gas jet containing suspended particles impinges on a flat plate; particles of sufficiently large inertia are deposited on the plate, while smaller particles are carried on with the flowing gas. A stage efficiency, E, is defined as the fraction of particles entering the *stage* that are collected on the plate. E can range between

zero (no particles are collected) and one (all particles are collected). The collection efficiency of an ideal impactor stage would be a step function, for which all particles smaller than some critical size pass through, while those larger than this size are collected. Practically, boundary layer and centerline effects result in the S–shaped efficiency curves that are predicted theoretically (*e.g.*, Rader and Marple, 1985) and observed experimentally (*e.g.*, Rubow *et al.*, 1987). The stage efficiency depends on the impactor geometry, flow rate, gas properties (density and viscosity), and particle properties (diameter, density, shape factor, and slip correction).

A cascade impactor consists of a series of single–stage impactors, where each subsequent stage collects progressively smaller particles. A stage response,[1] K_i, is defined as the fraction of particles entering the *impactor* that are collected on the i^{th} stage. The i^{th} stage response is obtained as the product of its efficiency, E_i, and terms describing the fraction of particles that are neither lost on walls nor collected on previous stages. Neglecting particle losses within an impactor operating at a specific flow rate, the following expressions for stage responses can be written (*see also* Puttock, 1981 or Crump and Seinfeld, 1982a):

$$\begin{aligned} K_1(d_{pa}) &= E_1(d_{pa}) \\ K_i(d_{pa}) &= E_i(d_{pa})(1-E_{i-1}(d_{pa}))\cdots(1-E_1(d_{pa})) \qquad i = 2, \ldots, n \end{aligned} \tag{1}$$

where the aerodynamic diameter,[2] d_{pa}, is introduced. Particles with equal aerodynamic diameters will behave essentially the same in an impactor, independent of their particular density, shape factor, or slip correction (Rader and Marple, 1985). With losses neglected, the stage response for the first stage is identical to its stage efficiency, while the stage responses for subsequent stages (with ideal, step–function efficiency functions) appear as sharp–sided top–hat functions. Due to losses and to the S–shaped nature of stage efficiency curves, however, experimentally observed stage response curves deviate from this ideal top–hat shape, and instead appear Gaussian in shape.

The expected stage mass loadings, M_i, can be described by the following integral expression:

$$M_i = \int K_i(d_{pa}) f(d_{pa}) dd_{pa} \tag{2}$$

---

[1]The stage response function is also called the kernel function.

[2]The aerodynamic diameter is the diameter of the unit density ($\rho_p = 1$ g/cm^3) sphere that has the same settling velocity as the particle.

where $f(d_{pa})$ is the mass distribution defined so that $f(d_{pa})dd_{pa}$ is the mass of particles entering the impactor with diameters between d_{pa} and $d_{pa}+dd_{pa}$. Given the response functions $K_i(d_{pa})$, the inversion problem amounts to determining which inlet distribution $f(d_{pa})$ gives the best agreement with the measured data set M_i. A variety of such algorithms is available in the literature (*e.g.*, Twomey, 1975; Raabe, 1978; Puttock, 1981; Crump and Seinfeld, 1982a,b; Markowski, 1987, 1988; and Wolfenbarger and Seinfeld, 1988).

The choice of a data inversion method can influence the requirements for the stage response function. For example, the histogram method is still frequently used. This method assumes an ideal impactor, for which each stage has a characteristic cutoff size which is usually approximated by its d_{p50} (the aerodynamic diameter for which 50% of the particles approaching the stage are collected). The mass collected on a stage is assumed to come from particles with aerodynamic diameters larger than its cut–off, but smaller than the cut–off of the previous stage. For impactors with sharp, well spaced cutoffs and low interstage losses, this technique works well. Complete stage response functions are not required in this case, instead the single–stage efficiency curves are used to determine the stage cutoffs. With the histogram method in mind, the results from cascade impactor calibrations are frequently presented as single–stage efficiency curves.

Inversion algorithms that include the integration of Equation 2 require that the complete response function for each stage be specified. In demonstrating their inversion method, Crump and Seinfeld (1982a) neglected losses and formed each $K_i(d_{pa})$ from the theoretical, universal efficiency curves of Marple and Liu (1974). Puttock (1981) constructed response functions based on Rao and Whitby's (1977, 1978) experimental data, although further assumptions were required to describe stages that were not characterized by Rao and Whitby. Knuth (1984) presented his calibration results for a Sierra 235 cascade impactor in terms of stage response functions; losses were measured but were not presented with the results.

In the present study, the calibration method is designed to provide direct measurement of the stage response functions whenever possible. By operating the impactor as a fully assembled unit, interstage effects on both stage collection efficiencies and losses are properly accounted for.

3 Experimental Methods

The Andersen Mark III cascade impactor used in the present study is a multistage, multinozzle instrument that aerodynamically classifies aerosol samples. The main

assembly (see Figure 1) consists of eight multinozzle collection stages (numbered 0 through 7) and a backup filter; in our test configuration the unit is preceded by a single–nozzle preimpactor (see Figure 2). Table 1 summarizes the operating parameters for the impactor at 14.4 ALPM (actual liters per minute at $P_{ambient}$ = 630 mm Hg, $T_{ambient}$ = 22° C), the flowrate used throughout this study. A critical orifice was used for flow regulation; the flowrate through the impactor was checked with a mass flow meter before each test. All data reported here were obtained with the impactor operated in a vertical orientation with the inlet at the top.

For the multiple–nozzle stages, the jet diameter indicated in Table 1 is the measured average for ten randomly selected nozzles: observed diameter variations between the nozzles for a particular stage were at most one percent. Note that the jet velocity for stage 7 includes a density correction; pressure drops through earlier stages are small enough that density corrections can be neglected. Jet Reynolds numbers ($Re = \rho VD/\mu$) are also shown. Untreated, precut glass–fiber impaction substrates as shown in Figure 1 were used.

Table 1. Stage Parameters for the Andersen Mark III Cascade Impactor at 14.4 ALPM ($\rho = 9.86 \cdot 10^{-4}$ g/cm^3, $\mu = 1.83 \cdot 10^{-4}$ g/(cm·s))

Stage No.	No. of Jets	Orifice Diameter D (cm)	Reynolds Number Re	Jet Velocity V (m/sec)	Cut–Point Diameter $d_{p50}(\mu m)$
PI	1	1.23	1339	2.0	10.7
0	264	.162	38	0.4	13.7
1	264	.122	51	0.8	10.5
2	264	.0916	68	1.4	6.62
3	264	.0744	84	2.1	4.88
4	264	.0548	114	3.9	2.80
5	264	.0362	172	8.8	1.42
6	264	.0270	231	16.	0.65
7	156	.0259	407	30.	——

Calibration test aerosols were generated with the Vibrating Orifice Aerosol Generator (VOAG)(Model 3450, TSI Inc., St. Paul, MN), which relies on the uniform, periodic breakup of a liquid jet to create monodisperse droplets (Berglund and Liu, 1973). One drawback with using VOAG–generated calibration aerosol is that coagulation can result in

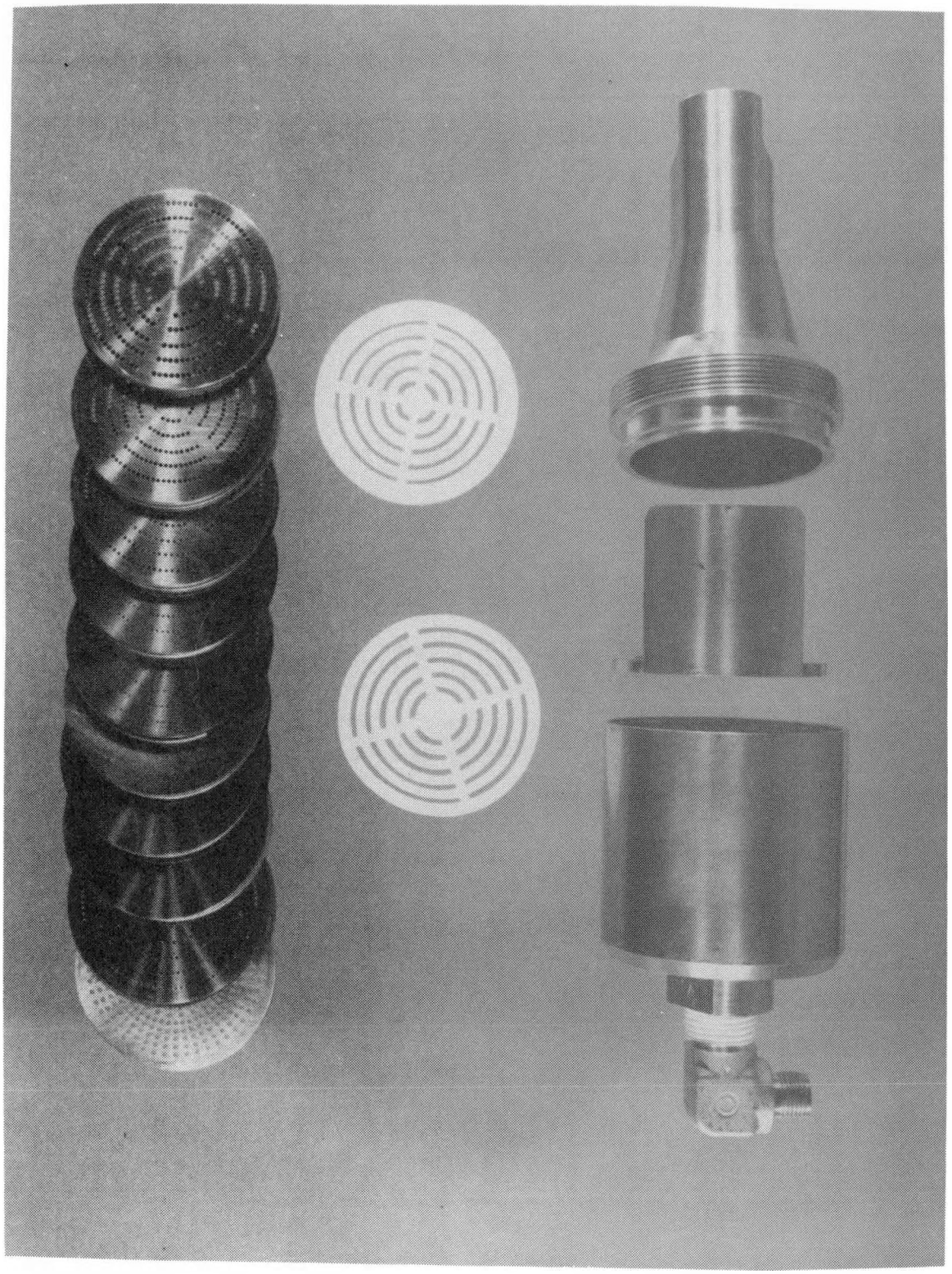

Figure 1. Andersen Mark III cascade impactor.

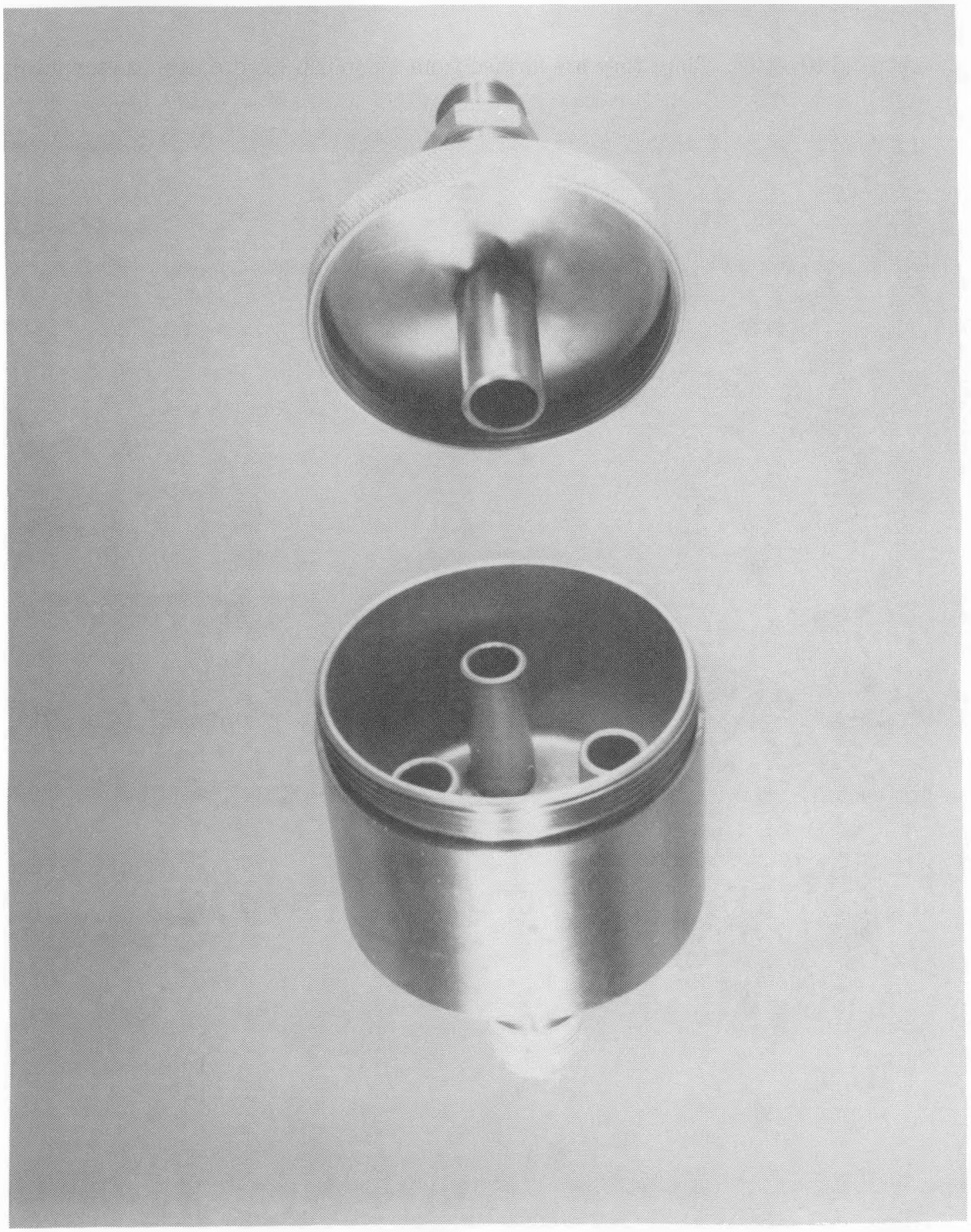

Figure 2. Single–nozzle preimpactor for the Andersen Mark III cascade impactor.

multiplet populations. Since they are formed from monodisperse droplets, these multiplets have diameters that can be accurately calculated, *i.e.*, a doublet would have a diameter equal to the cube–root of two (1.26) times the singlet diameter. Singlet and multiplet concentrations were continuously measured during the tests with an Aerodynamic Particle Sizer (APS)(Model 33B, TSI Inc.), so that the multiplet contribution to the impactor response data could be accounted for. Droplets were generated from solutions of oleic acid in isopropyl alcohol; the size of the oleic–acid droplet after the alcohol evaporates was calculated from the solution concentration and from the operating parameters of the VOAG. The droplets were brought to a Boltzmann charge equilibrium by exposure to a bipolar ion cloud generated by a ^{210}Po radioactive source. Sufficient residence time allowed the alcohol to evaporate before the droplets were drawn into the impactor. The density of the oleic acid droplets was 0.895 g/cm^3.

For diameters between 1.3 and 20 μm, a fluorometric method was used. In this method, the droplets are tagged with trace amounts of a fluorescent dye (uranine) and introduced into the impactor. After the test, the impactor was disassembled: oleic acid/uranine deposits on each glass–fiber substrate and on the after–filter were dissolved with metered quantities of an aqueous solution of 0.001 N sodium hydroxide. Particle collection by the preimpactor was determined by washing the bottom and inside of the collection cup, as well as the outer surfaces of the three vent tubes (see Figure 2). All other internal surfaces were washed to account for total losses. Only particles which passed the exit plane of the preimpactor nozzle were considered to have entered the impactor; losses within the inlet to the preimpactor were considered to be sampling losses and were not considered. The relative fluorescence of each wash was measured with a fluorometer (Model 112, Turner Associates, Palo Alto, CA). With proper choice of dilutions, all solutions could be measured on the same fluorometer scale, for which the instrument response is linear with uranine concentration.

From the measured uranine concentration and the volume of diluent, the mass of uranine in the wash was obtained, which is proportional to the mass of deposited droplets. The total mass of aerosol entering the impactor was obtained as the sum of all the stage deposits, the filter deposit, and the total losses; a stage response was calculated as the ratio of the mass collected on the stage to the total mass. For each test, all stage responses and the total mass were adjusted to account for the multiplet concentration as measured by the APS (Marple *et al.*, 1987). Doublets were typically found to account for about 6% of the total mass, while higher multiplets were rarely observed.

The generation of particles with diameters between 0.8 and 1.3 μm required such low concentrations of oleic acid (and uranine) that the sampling times required to obtain accurate fluorescence measurements became too long. Since the particle losses in this size range are low, it was possible to use an alternate calibration approach in which two impactors are set up in parallel. In the first, all plates below the nozzle–plate of interest are removed from a fully assembled impactor. In the second, a collection plate is included beneath the nozzle–plate of interest, and all following plates are again removed. Using the APS, the concentration ratio of particles exiting the second impactor to those exiting the first gives the number of particles collected for the stage of interest. In the absence of losses, the response function is obtained by dividing this value by the concentration measured upstream of the impactors. For the small diameters used in this method, losses were less than a few percent.

Since the generation of particles smaller than 1.3 μm requires the use of dilute solutions of oleic acid in alcohol, the concentration of impurities begins to affect the accuracy with which the droplet diameter can be determined. By comparing the APS response for these particles with that for PSL (polystyrene latex) monodisperse spheres (Duke Scientific, Menlo Park, CA) and for particles in the overlapping size range from stronger solutions, it was possible to estimate these impurities for each test. The measured range of impurities was 5 to 15 ppm. Although particle diameters have been corrected for impurities, uncertainties for particle diameters less than about 1.3 μm are greater than for larger sizes. The estimated uncertainties in diameter are 3% for particles below 1.3 μm in size, and 2% for particles above 1.3 μm. The presence of impurities limited the present study to particles above about 0.7 μm. Thus, no information was obtained beyond stage 6.

4 Experimental Stage Response Function

The experimental stage response functions, K_i, for the preimpactor and stages 0 and 1 are shown in Figure 3; total losses and the response functions for the preimpactor and stages 2 through 6 are shown in Figure 4. The symbols indicate experimental data, while the solid curves are semi–empirical fits (see Section 5). Data obtained with both the fluorometric and concentration–ratio techniques are shown, and are seen to be in good agreement where the techniques overlap. The preimpactor curve displays the classical S–shape since, as the first collection surface encountered by the aerosol, the preimpactor stage efficiency and stage response are identical. Later stages show bell–shaped stage responses that arise from the interaction of their nonideal collection efficiencies and those of earlier stages.

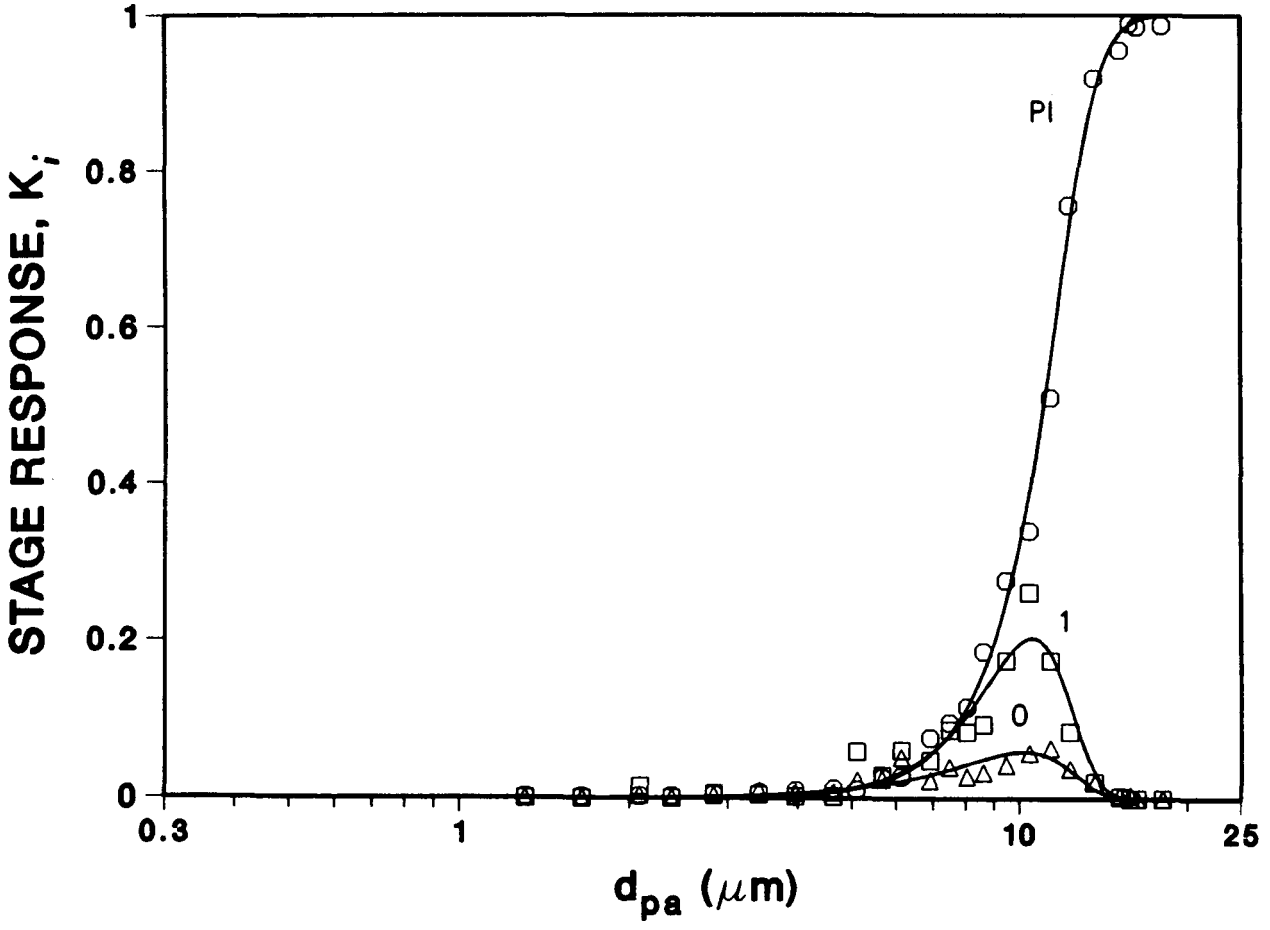

Figure 3. Stage response function for an Andersen Mark III impactor – preimpactor (PI), stages 0 and 1.

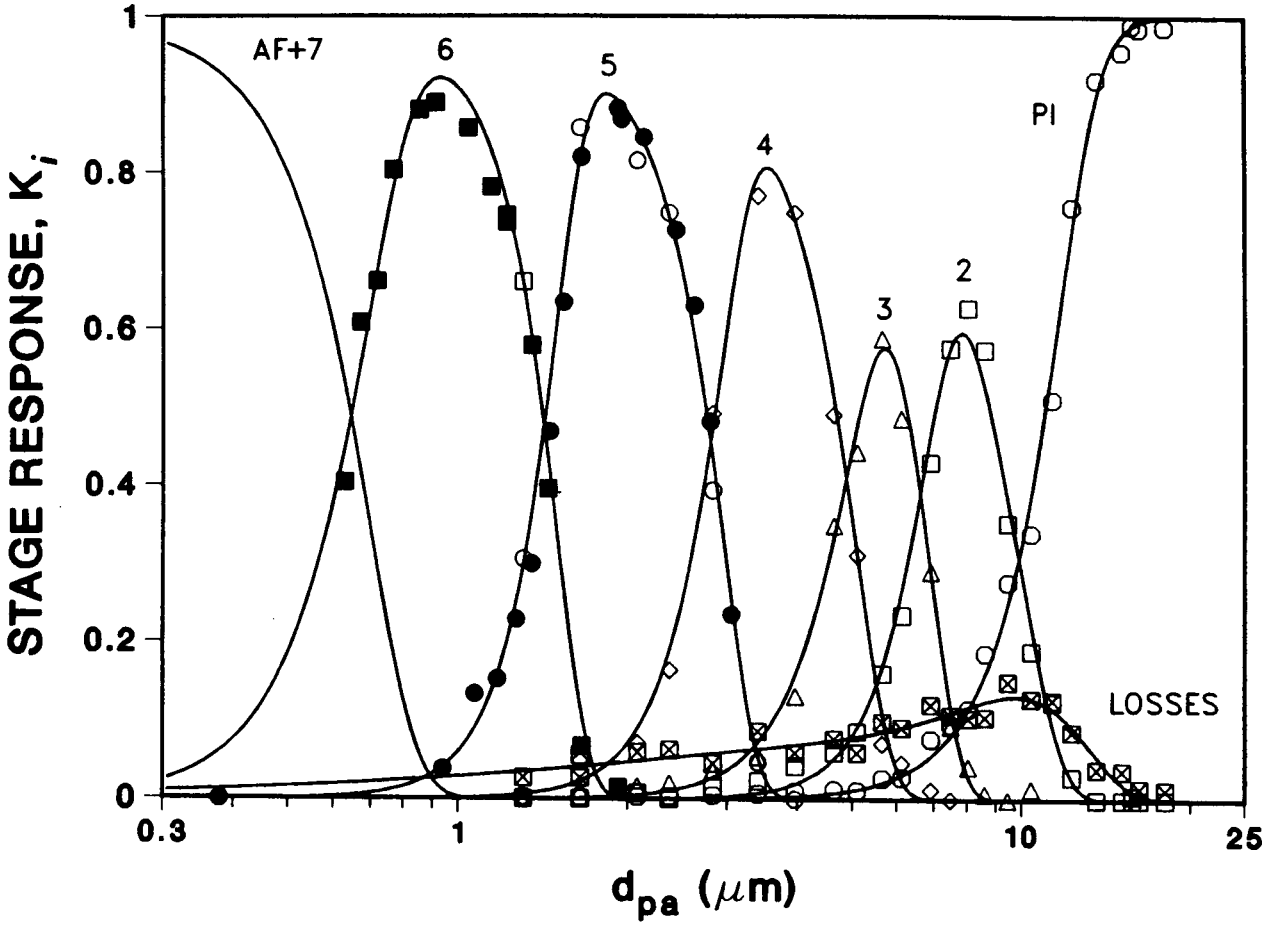

Figure 4. Stage response function for an Andersen Mark III impactor – preimpactor (PI), losses, stages 2 through 6, and the sum of stage 7 and the after filter (AF+7). Filled symbols from ratio technique, open symbols from fluorescent technique.

The presence of the preimpactor has a dramatic effect on stages 0 and 1. As will be shown later, the d_{p50} for the preimpactor is essentially equal to that for stage 1, and is actually less than the d_{p50} of stage 0. The maximum response of stage 1 is less than 20%, while no more than 5% of the aerosol entering the impactor is ever found on stage 0. The preimpactor efficiency curve does not show a sharp cutoff, so that its presence is also felt (although to a lesser extent) by stages 2 through 4. The estimate for the preimpactor d_{p50} obtained in this work (10.9 μm at 14.4 ALPM) agrees well with that found by McFarland *et al.* (1978) (10.8 μm at 14.2 ALPM).

Internal losses and the S–shaped responses of the stages result in maximum stage responses that fall significantly short of unity. The maximum response of stages 2 and 3 is only 0.6, while stages 4, 5, and 6 show somewhat higher maximums (0.8 to 0.9). Physically, maxima less than unity indicate that a monodisperse aerosol is never collected exclusively on one stage, but is distributed among several stages and internal losses.

Interstage losses reached a maximum of about 15% for particle aerodynamic diameters of about 10 μm, decreasing for both larger and smaller sizes. The decrease in losses for particles smaller than 10 μm has been frequently observed, and results from the decrease with size of both major loss mechanisms (inertial and gravitational deposition). Diffusional and electrical deposition, which increases for smaller particles, are not significant in this study (particle diameters greater than 0.7 μm). The decrease in losses for particles larger than 10 μm is not typically observed, and results from our definition that a particle enters the impactor only by passing the exit plane of the preimpactor nozzle. Particles that pass the nozzle exit plane see no surfaces until the impaction surface, where they are collected with unit efficiency in the large–particle limit. By this definition, particle losses approach zero in the large–particle limit, as confirmed by experiment. Particle deposition certainly occurs in the preimpactor nozzle (and in upstream plumbing), but these losses are considered issues of particle sampling and transport. Aerosol sampling and transport mechanisms have been extensively studied, and a review of this work (Fissan and Schwientek, 1987) has recently been published. A computer code (ASTEC) for calculating sampling and transport efficiencies has recently become available (Yamano and Brockmann, 1988).

5 Analytic Representation of Stage Response Functions

As discussed above, the reconstruction of a continuous size distribution from a set of stage–deposit data requires the use of an inversion algorithm. The stage–response and interstage–loss data shown in Figures 3 and 4 provide the complete characterization of the

Mark III cascade impactor (for liquid droplets) required for such an analysis. Generally, the inversion problem amounts to using Equation 2 to determine which inlet distribution, $f(d_{pa})$, gives the best agreement with the measured data set, M_i. The integration required in Equation 2 would be greatly simplified if an analytic representation of the data could be found. Such a representation is presented in this section.

The present analysis is based on the expressions for stage response given in Equation 1 where interstage losses have been neglected. In order to use this formulation, an interstage–loss function, $L(d_{pa})$ (defined as the fraction of particles of size d_{pa} lost in the impactor) is introduced and applied immediately to the inlet distribution. Reducing the inlet distribution by the measured interstage losses is obviously nonphysical, since these losses occur throughout the impactor. This assumption greatly simplifies the analysis and yet, as shown below, satisfies our primary goal by providing an acceptable fitting of the stage–response data. Under this assumption, Equation 2 can be expressed as:

$$M_i = \int K_i(d_{pa}) f^*(d_{pa}) dd_{pa}$$

where:

$$\begin{aligned} f^*(d_{pa}) &= f(d_{pa})(1-L(d_{pa})) \\ K_{\mathrm{PI}}(d_{pa}) &= E_{\mathrm{PI}}(d_{pa}) \\ K_i(d_{pa}) &= E_i(d_{pa})(1-E_{i-1}(d_{pa}))\cdots(1-E_{\mathrm{PI}}(d_{pa})) \quad i = 0, 1,..., 7 \\ K_{\mathrm{AF}}(d_{pa}) &= (1-E_7(d_{pa}))(1-E_6(d_{pa}))\cdots(1-E_{\mathrm{PI}}(d_{pa})). \end{aligned} \tag{3}$$

K_{PI} is the response function for the preimpactor, and K_i are the response functions for stages 0 through 7. The response K_{AF} describes the behavior of the after–filter following stage 7, which is assumed to collect with unit efficiency all of the particles exiting stage 7.

Analytic representations for both L and the S–shaped stage–efficiency curves are needed to complete the analysis. After investigating a variety of efficiency functions, the following form provided sufficient flexibility in fitting the data:

$$E_i(d_{\mathrm{pa}}) = \tanh\left[\left[\frac{d_{\mathrm{pa}}}{a_{\mathrm{i}}}\right]^{b_{\mathrm{i}}}\right] \tag{4}$$

where a_{i} and b_{i} are parameters for each stage that are fit to the experimental data using

the least–squares minimization algorithm discussed below. The correlation of Equation 4 provides the expected efficiency limits: unit efficiency for infinitely large particles, and zero efficiency for infinitesimally small particles. The cut–point diameter is easily shown to be $d_{p50} = a_i(0.5493)^{1/b_i}$.

The experimentally observed losses can be described with the following empirical form:

$$L(d_{pa}) = (0.361y - 0.732y^2 + 0.719y^3) \cdot exp(-y^{3.88}) \qquad (5)$$

where $y = d_{pa}/10.57$

and the constants are the fitted parameters obtained using the least–squares minimization method discussed below. Equation 5 tends to zero in both the large and small particle limits.

The parameters given in Equations 4 and 5 were found by minimizing the sum–of–squares differences between the experimental data (K_i and L) and the responses predicted with Equations 3–5. A gradient–expansion, nonlinear least–squares minimization algorithm presented in Bevington (1969) was used to perform the fitting. The present analysis used a two–step fitting process. First, the loss response function parameters were obtained by fitting Equation 5 to the measured losses: these parameters have already been given in Equation 5. Second, all eight of the stage response curves were fit simultaneously using the expressions for K_i in Equation 3, the correlation formula for E_i in Equation 4, the measured K_i data, and the fitted results for L from the previous step.[3] Table 2 presents the fitted parameters (a_i and b_i) obtained with this analysis.

The fitted approximations for K_i are shown as solid curves in Figures 3 and 4. As can be seen, the agreement with data is quite good. The maximum observed deviations between experimental and fitted response functions is 6.7% of full scale, with typical deviations of about 3% of full scale. Both the maximum and typical deviations are consistent with estimates of experimental uncertainty, and thus the proposed analytic expressions for the K_i are sufficiently accurate for use in the inversion of Equation 2.

Traditional cut–point diameters for the stages can be found by solving Equation 4 for d_{pa} with $E_i = 0.5$. Cut–point diameters obtained in this way are given in Table 1.

---

[3]The techniques used in this study did not allow calibration of stage 7. In our field work, the masses deposited on the after–filter and on stage 7 are combined, and an effective response function, $K_{7+AF} = (1-E_6)\cdots(1-E_{PI})$, is introduced for data analysis.

Table 2. Fitted Parameters for the Andersen Mark III Cascade Impactor at 14.4 ALPM
$\rho = 9.86 \cdot 10^{-4}$ g/cm^3, $\mu = 1.83 \cdot 10^{-4}$ g/(cm·s)

Stage No.	a_i	b_i
PI	12.08	4.987
0	20.93	3.000
1	11.88	4.894
2	7.275	6.361
3	5.447	5.409
4	3.104	5.877
5	1.566	6.204
6	0.7465	4.124

6 Particle Bounce

Attempts to apply the present calibration study to interpretation of solid–particle data should proceed with caution. The results of several investigators (*e.g.*, Rao and Whitby, 1977, 1978; Knuth, 1984; and Vanderpool *et al.*, 1987) show that while glass–fiber substrates reduce particle bounce when compared to untreated surfaces, they do not eliminate it. Vanderpool *et al.* (1987) give evidence that even silicone–sprayed glass–fiber filters show significant bounce effects; interestingly, stainless–steel foils coated with the same spray showed no evidence of bounce. The use of other substrates, such as greased foils, would likely require a recalibration of the impactor.[4]

7 Conclusions

This document presents an experimental determination of the stage responses for an Andersen Mark III cascade impactor. The calibration method was designed so as to provide direct measurement of the stage response functions whenever possible. By operating the impactor as a fully assembled unit, inter–stage effects on both stage collection efficiencies and losses are reliably accounted for. Internal losses and the S–shaped collection efficiencies of the stages result in maximum stage responses that fall

[4]Collection efficiencies of glass–fiber substrates have been shown to differ markedly from oil–coated stainless steel plates. See Rao and Whitby (1977).

significantly short of unity. Physically, maxima less than unity indicate that a monodisperse aerosol is never collected exclusively on one stage, but is distributed among several stages and internal losses. Also, the presence of the preimpactor has a dramatic effect on stages 0 and 1, limiting their maximum responses to 0.2 and 0.05, respectively.

An analytic representation based on the response data is introduced; this continuous correlation will be helpful in inversion methods that rely on the integral response function given in Equation 2. The advantages associated with such inversions (as compared to simple histogram methods) depend on the nature of the aerosol being sampled, and have not been explored in this work. As the response curves obtained in this work strictly apply only for liquid particles, their use with solid–particle systems should be approached with caution.

8 References

Berglund, R.N. and Liu, B.Y.H. (1973) "Generation of Monodisperse Aerosol Standards," *Environ. Sci. Technol.* 7:147–153.

Bevington, P.R. (1969) *Data Reduction and Error Analysis for the Physical Sciences*, McGraw–Hill, New York.

Crump, J.G. and Seinfeld, J.H. (1982a) "A New Algorithm for Inversion of Aerosol Size Distribution Data," *Aerosol Sci. Technol.* 1:15–34.

Crump, J.G. and Seinfeld, J.H. (1982b) "Further Results on Inversion of Aerosol Size Distribution Data: Higher–Order Sobolev Spaces and Constraints," *Aerosol Sci. Technol.* 1:363–369.

Fissan, H. and Schwientek, G. (1987) "Sampling and Transport of Aerosols," *TSI J. Particle Instrumentation* 2(2):3–10, TSI Inc., St. Paul, MN.

Knuth, R.H. (1984) "Calibration and Field Application of a Sierra Model 235 Cascade Impactor," *Am. Ind. Hyg. Assoc. J.* 45:393–398.

Markowski, G.R. (1987) "Improving Twomey's Algorithm for Inversion of Aerosol Measurement Data," *Aerosol Sci. Technol.* 7:127–141.

Markowski, G.R. (1988) "Inverting Ill–Conditioned Aerosol Data: Improvements to STWOM," Amer. Assoc. Aerosol Research. 1988 Annual Meeting, Chapel Hill, NC, October 10–14.

Marple, V.A. and Liu, B.Y.H. (1974) "Characteristics of Laminar Jet Impactors," *Environ. Sci. Technol.* 8:648–654.

Marple, V.A., Rubow, K.L., Turner, W., Spengler, J.D. (1987) "Low Flow Rate Sharp Cut Impactors for Indoor Air Sampling: Design and Calibration," *J. Air Pollut. Control* 37:1303–1307.

McFarland, A.R., Ortiz, C.O., and Bertch, R.W. (1978) "A High Capacity Preseparator for Collecting Large Particles," presented at Am. Ind. Hyg. Assoc. Annual Meeting, Los Angeles, CA, May, 1978.

Puttock, J.S. (1981) "Data Inversion for Cascade Impactors: Fitting Sums of Log–Normal Distributions," *Atmos. Environ.* 15:1709–1716.

Raabe, O.G. (1978) "A General Method for Fitting Size Distributions to Multicomponent Aerosol Data Using Weighted Least–Squares," *Environ. Sci. Technol.* 12:1162–1167.

Rader, D.J. and Marple, V.A. (1985) "Effect of Ultra–Stokesian Drag and Particle Interception on Impaction Characteristics," *Aerosol Sci. Technol.* 4:141–156.

Rao, A.K. and Whitby, K.T. (1977) "Nonideal Collection Characteristics of Single Stage and Cascade Impactors," *Am. Ind. Hyg. Assoc. J.* 38:174–179.

Rao, A.K. and Whitby, K.T. (1978) "Non–Ideal Collection Characteristics of Inertial Impactors – II. Cascade Impactors," *J. Aerosol Sci.* 9:87–100.

Rubow, K.L., Marple, V.A., Olin, J., and McCawley, M.A. (1987) "A Personal Cascade Impactor: Design, Evaluation and Calibration," *Am. Ind. Hyg. Assoc. J.* 48:532–538.

Twomey, S. (1975) *J. Comput. Phys.* 18:188–200.

Vanderpool, R.W., Lundgren, D.A., Marple, V.A., and Rubow, K.L. (1987) "Cocalibration of Four Large–Particle Impactors," *Aerosol Sci. Technol.* 7:177–185.

Wolfenbarger, J.K. and Seinfeld, J.H. (1988) "Inversion of Aerosol Size Distribution Data Using Constrained Regularization," Amer. Assoc. Aerosol Research. 1988 Annual Meeting, Chapel Hill, NC, October 10–14.

Yamano, N. and Brockmann, J.E. (1989) "Aerosol Sampling and Transport Efficiency Calculation (ASTEC) Code Version 1.0: Code Description and User's Manual," SAND88–1447.

Distribution:
UC-2 (111)

Inhalation Toxicology Research Institute (4)
Lovelace Biomedical and Environmental
Research Institute
Albuquerque, NM 87115
Attn:
Y.S. Cheng
M. Hoover
G.J. Newton
H.C. Yeh

V.A. Marple
University of Minnesota
Department of Mechanical Engineering
Minneapolis, MN 55455

AEE Winfrith (2)
Dorchester, Dorset DT2 8DH
England
Attn:
J.P. Mitchell
A. Nichols

U.S. Nuclear Regulatory Commission (2)
Office of Nuclear Regulatory Research
Division of Systems Research
Accident Evaluation Branch
Washington, DC 20555
Attn:
P. Worthington
B. Burson

Argonne National Laboratory (2)
9700 South Cass
Argonne, IL 60439
Attn:
K.H. Leong
J. Frink

Oak Ridge National Laboratory (2)
P.O. Box X
Oak Ridge, TN 37831
Attn:
A.L. Wright
T. Kress

Battelle Institute (2)
505 King Avenue
Columbus, OH 43201
Attn:
K.W. Lee
J. Gieseke

Sandia Internal:

1510	J.W. Nunziato
1511	D.K. Gartling
1511	L.A. Mondy (5)
1512	J.C. Cummings
1512	D.A. Benson
1512	D.J. Rader (15)
1513	D.W. Larson
1520	L.W. Davison
1530	D.B. Hayes
1550	C.W. Peterson
3141	S.A. Landenberger (5)
3141–1	C.L. Ward (8) for DOE/OSTI
3151	W.I. Klein (3)
5214	W.F. Hartman
5214	B.A. Boughton
6321	R.E. Luna
6321	B.D. Zak
6321	N.R. Grandjean
6321	H.W. Church
6400	D.J. McCloskey
6422	D.A. Powers
6422	J.E. Brockmann (15)
6422	D.A. Lucero (2)
6422	M.D. Allen
6429	F. Gelbard
8524	J.A. Wackerly
9113	C.M. Craft